Expressions for the nonlinear transmission performance of multi-mode optical fiber

A. D. Ellis,[1,*] N. Mac Suibhne,[2] F. C. Garcia Gunning[2] and S. Sygletos[1]

[1]*Aston Institute of Photonic Technology, Aston University, Birmingham B4 7ET, England*
[2]*Tyndall National Institute, Lee Maltings, Dyke Parade, Cork, Ireland*
[*]*andrew.ellis@aston.ac.uk*

Abstract: We develop an analytical theory which allows us to identify the information spectral density limits of multimode optical fiber transmission systems. Our approach takes into account the Kerr-effect induced interactions of the propagating spatial modes and derives closed-form expressions for the spectral density of the corresponding nonlinear distortion. Experimental characterization results have confirmed the accuracy of the proposed models. Application of our theory in different FMF transmission scenarios has predicted a ~10% variation in total system throughput due to changes associated with inter-mode nonlinear interactions, in agreement with an observed 3dB increase in nonlinear noise power spectral density for a graded index four LP mode fiber.

OCIS codes: (060.0060) Fiber optics and optical communications; (060.4370) Nonlinear optics, fibers.

References and links

1. P. J. Winzer, "Optical Networking Beyond WDM," IEEE Photon. J. **4**(2), 647–651 (2012).
2. D. J. Richardson, "Applied physics. Filling the light pipe," Science **330**(6002), 327–328 (2010).
3. A. D. Ellis, "The MODE-GAP project," in Proceedings of Frontiers in Optics Conference, 2012 OSA Technical Digest Series (Optical Society of America, 2012), paper, FW1D.
4. F. Poletti, N. V. Wheeler, M. N. Petrovich, N. Baddela, E. N. Fokoua, J. R. Hayes, D. R. Gray, Z. Li, R. Slavík, and D. J. Richardson, "Towards high-capacity fibre optic communications at the speed of light in vacuum," Nat. Photonics **7**(4), 279–284 (2013).
5. V. A. J. M. Sleiffer, Y. Jung, V. Veljanovski, R. G. H. van Uden, M. Kuschnerov, H. Chen, B. Inan, L. G. Nielsen, Y. Sun, D. J. Richardson, S. U. Alam, F. Poletti, J. K. Sahu, A. Dhar, A. M. J. Koonen, B. Corbett, R. Winfield, A. D. Ellis, and H. de Waardt, "73.7 Tb/s (96 x 3 x 256-Gb/s) mode-division-multiplexed DP-16QAM transmission with inline MM-EDFA," Opt. Express **20**(26), B428–B438 (2012).
6. Y. Yang, Y. Yan, N. Ahmed, Y. Jeng-Yuan, L. Zhang, Y. Ren, H. Huang, K. M. Birnbaum, B. I. Erkmen, S. Dolinar, M. Tur, and A. E. Willner, "Mode properties and propagation effects of optical orbital angular momentum (OAM) modes in a ring fiber," IEEE Photon. J. **4**(2), 535–543 (2012).
7. P. J. Winzer and G. J. Foschini, "MIMO capacities and outage probabilities in spatially multiplexed optical transport systems," Opt. Express **19**(17), 16680–16696 (2011).
8. R. Pini, R. Salimbeni, A. F. M. Y. Haider, M. Matera, and C. Lin, "Continuously tunable multiple-order stimulated four-photon mixing in a multimode silica fiber," Opt. Lett. **9**(3), 79–81 (1984).
9. R.-J. Essiambre, R. Ryf, M. A. Mestre, A. H. Gnauck, R. Tkach, A. Chraplyvy, S. Randel, Y. Sun, X. Jiang, and R. Lingle, "Inter-modal nonlinear interactions between well separated channels in spatially-multiplexed fiber transmission," in Proceedings of European Conference on Optical Communication (ECOC 2012), Amsterdam, paper Tu.1.C.4, (2012).
10. N. Mac Suibhne, R. Watts, S. Sygletos, F. C. Garcia Gunning, L. Grüner-Nielsen, and A. D. Ellis, "Nonlinear Pulse Distortion in Few-Mode Fiber," in Proceedings of European Conference on Optical Communication (ECOC 2012), paper Th.2.F.5, (2012).
11. R. Essiambre, M. A. Mestre, R. Ryf, A. H. Gnauck, R. W. Tkach, A. R. Chraplyvy, Y. Sun, X. Jiang, and R. Lingle, "Experimental observation of inter-modal cross-phase modulation in few-mode fibers," IEEE Photon. Technol. Lett. **25**(6), 535–538 (2013).
12. R. Essiambre, M. A. Mestre, R. Ryf, A. H. Gnauck, R. W. Tkach, A. R. Chraplyvy, Y. Sun, X. Jiang, and R. Lingle, "Experimental investigation of inter-modal four-wave mixing in few-mode fibers," IEEE Photon. Technol. Lett. **25**(6), 539–542 (2013).
13. F. Ferreira, S. Jansen, P. Monteiro, and H. Silva, "Nonlinear semi-analytical model for simulation of few-mode fiber transmission," IEEE Photon. Technol. Lett. **24**(4), 240–242 (2012).

#193496 - $15.00 USD Received 8 Jul 2013; revised 15 Sep 2013; accepted 16 Sep 2013; published 20 Sep 2013

14. S. Mumtaz, R.-J. Essiambre, and G. P. Agrawal, "Nonlinear propagation in multimode and multicore fibers: generalisation of the Manakov equations," J. Lightwave Technol. **31**(3), 398–406 (2013).
15. A. Mecozzi, C. Antonelli, and M. Shtaif, "Coupled Manakov equations in multimode fibers with strongly coupled groups of modes," Opt. Express **20**(21), 23436–23441 (2012).
16. D. Rafique, S. Sygletos, and A. D. Ellis, "Impact of power allocation strategies in long-haul few-mode fiber transmission systems," Opt. Express **21**(9), 10801–10809 (2013).
17. P. P. Mitra and J. B. Stark, "Nonlinear limits to the information capacity of optical fibre communications," Nature **411**(6841), 1027–1030 (2001).
18. A. D. Ellis, J. Zhao, and D. Cotter, "Approaching the Non-linear Shannon Limit," J. Lightwave Technol. **28**(4), 423–433 (2010).
19. X. Chen and W. Shieh, "Closed-form expressions for nonlinear transmission performance of densely spaced coherent optical OFDM systems," Opt. Express **18**(18), 19039–19054 (2010).
20. A. D. Ellis and N. J. Doran, "Are few mode fibres.a practical solution to the capacity crunch", in Proceedings of 15th International Conference on Transparent Optical Networks (ICTON 2013), paper TuC2.1 (2013).
21. G. Bosco, P. Poggiolini, A. Carena, V. Curri, and F. Forghieri, "Analytical results on channel capacity in uncompensated optical links with coherent detection," Opt. Express **19**(26), B440–B449 (2011).
22. P. Poggiolini, A. Carena, V. Curri, G. Bosco, and F. Forghieri, "Analytical Modeling of Non-Linear Propagation in Uncompensated Optical Transmission Links," IEEE Photon. Technol. Lett. **23**(11), 742–744 (2011).
23. R. Essiambre, G. Kramer, P. J. Winzer, G. J. Foschini, and B. Goebel, "Capacity limits of optical fiber networks," J. Lightwave Technol. **28**(4), 662–701 (2010).
24. D. Rafique and A. D. Ellis, "Impact of signal-ASE four-wave mixing on the effectiveness of digital back-propagation in 112 Gb/s PM-QPSK systems," Opt. Express **19**(4), 3449–3454 (2011).
25. T. Tanimura, M. Nölle, J. K. Fischer, and C. Schubert, "Analytical results on back propagation nonlinear compensator with coherent detection," Opt. Express **20**(27), 28779–28785 (2012).
26. G. Rademacher, S. Warm, and K. Petermann, "Analytical description of cross modal nonlinear interaction in mode multiplexed multi-mode fibers," IEEE Photon. Technol. Lett. **24**(21), 1929–1932 (2012).
27. N. Mac Suibhne, A. D. Ellis, F. C. Garcia Gunning, and S. Sygletos, "Experimental verification of four wave mixing efficiency characteristics in a few mode fibre", in Proceedings of European Conference on Optical Communications (ECOC 2013), paper P1.14 (2013).
28. N. Bai, E. Ip, Y.-K. Huang, E. Mateo, F. Yaman, M. J. Li, S. Bickham, S. Ten, J. Liñares, C. Montero, V. Moreno, X. Prieto, V. Tse, K. Man Chung, A. P. Lau, H. Y. Tam, C. Lu, Y. Luo, G. D. Peng, G. Li, and T. Wang, "Mode-division multiplexed transmission with inline few-mode fiber amplifier," Opt. Express **20**(3), 2668–2680 (2012).
29. S. Randel, R. Ryf, A. H. Gnauck, M. A. Mestre, C. Schmidt, R. Essiambre, P. J. Winzer, R. Delbue, P. Pupalaikis, A. Sureka, Y. Sun, X. Jiang, and R. L. Lingle, "Mode-Multiplexed 6x20-GBd QPSK Transmission over 1200 km DGD-Compensated Few-Mode Fiber," in Optical Fiber Communication Conference, 2012 OSA Technical Digest Series (Optical Society of America, 2012), paper PDP5C.5.
30. E. Ip, M.-J. Li, Y.-K. Huang, A. Tanaka, E. Mateo, W. Wood, J. Hu, Y. Yano, and K. Koreshkov, "146 x6x19-Gbaud wavelength and mode-division multiplexed transmission over 10x50-km spans of few-mode fiber with a gain-equalised few-mode EDFA," in Optical Fiber Communication Conference, 2013 OSA Technical Digest Series (Optical Society of America, 2013), paper PDP5A.2.
31. R. Ryf, N. K. Fontaine, M. A. Mestre, S. Randel, X. Palou, C. Bolle, A. H. Gnauck, S. Chandrasekhar, X. Liu, B. Guan, R.-J. Essiambre, P. J. Winzer, S. G. Leon-Saval, J. Bland-Hawthorn, R. Delbue, P. Pupalaikis, A. Sureka, Y. Sun, L. Grüner-Nielsen, R. V. Jensen, and R. Lingle, "12 x 12 MIMO Transmission over 130-km Few-Mode Fiber;" in Proceedings of Frontiers in Optics Conference, 2012 OSA Technical Digest Series (Optical Society of America, 2012), paper FW6C.4.
32. T. Mori, T. Sakamoto, M. Wada, T. Yamamoto, and F. Yamamoto, "A low DMD four LP mode transmission fiber for wide-band WDM-MIMO system," in Proceedings of Optical Fiber Communication Conference, 2013 OSA Technical Digest Series (Optical Society of America, 2013), paper OTh3K.1.
33. G. P. Agrawal, *Nonlinear fiber optics*, (Springer Berlin, 2000).
34. A. D. Ellis and W. A. Stallard, "Four Wave mixing in ultra long transmission systems incorporating linear amplifiers", in Proceedings of IEE Colloquium on Non-Linear Effects in Fibre Communications, **159**, 6/1–6/4 (1990).
35. D. A. Cleland, A. D. Ellis, and C. H. F. Sturrock, "Precise modelling of four wave mixing products over 400km of step index fibre," Electron. Lett. **28**(12), 1171–1172 (1992).
36. P. D. Maker and R. W. Terhune, "Study of the optical effects due to an induced polarisation third order in the electric field strength," Phys. Rev. **137**(3A), A801–A818 (1965).
37. O. V. Sinkin, J.-X. Cai, D. G. Foursa, G. Mohs, and A. N. Pilipetskii, "Impact of broadband four-wave mixing on system characterisation," in Optical Fiber Communication Conference, 2013 OSA Technical Digest Series (Optical Society of America, 2013), paper OTh3G.
38. S. Kilmurray, T. Fehenberger, P. Bayvel, and R. I. Killey, "Comparison of the nonlinear transmission performance of quasi-Nyquist WDM and reduced guard interval OFDM," Opt. Express **20**(4), 4198–4205 (2012).
39. D. Rafique, S. Sygletos, and A. D. Ellis, "Impact of power allocation strategies in long-haul few-mode fiber transmission systems," Opt. Express **21**(9), 10801–10809 (2013).

#193496 - $15.00 USD Received 8 Jul 2013; revised 15 Sep 2013; accepted 16 Sep 2013; published 20 Sep 2013

40. B. Inan, B. Spinnler, F. Ferreira, D. van den Borne, A. Lobato, S. Adhikari, V. A. Sleiffer, M. Kuschnerov, N. Hanik, and S. L. Jansen, "DSP complexity of mode-division multiplexed receivers," Opt. Express **20**(10), 10859–10869 (2012).

1. Introduction

Multi-core and few-mode fiber (FMF) based systems are seen as a promising route to postpone the capacity crunch by increasing the number of modes used for communication without significantly changing the optical signal to noise ratio within each mode [1–3]. Various solutions are under investigation, including hollow core photonic band-gap fibers [4], few-mode fibers [5], and fibers supporting orbital angular momentum modes [6]. In order to support development of future systems based on these products, it is essential to understand both the linear and nonlinear transmission effects. Linear effects which restrict the performance of a few-mode fiber system include the orthogonality of mode multiplexers/demultiplexers and critically, in line mode dependent loss. A high mode dependent loss will result in unacceptably system outage [7], however for sufficiently low mode dependent loss, the system becomes unitary and the capacity scales with the number of modes. Preliminary measurements of nonlinearity of few-mode fibers have now commenced [8–12] and numerical models are now available [13–16] taking into account cross phase modulation such as inter mode nonlinear interactions. However, to the best of our knowledge, closed form expressions for the nonlinear Shannon limit of a FMF to those available for single mode fibers [17–19] are only beginning to emerge [20]. Such expressions are invaluable planning tools enabling simple scaling rules to be predicted and with subsequent experimental verification will provide important input to network operators and designers. Previous work has provided closed form expressions for single mode fiber for inter-channel nonlinear effects [19, 21, 22]. Strictly speaking, deterministic intra-channel nonlinearity may be compensated [23] leading to enhancements of a few dB. Similarly, for point to point links, inter-channel nonlinear effects may be compensated and the system becomes limited by the nonlinear interaction between signal and noise [24, 25]. In the context of multi-mode fiber, the compensation both inter and intra channel nonlinearity would be event more challenging than for single mode fibers, furthermore potential inter mode nonlinear interactions for a few-mode fiber have been identified [26].

In this paper we develop a simple, fully closed form expression for the nonlinear noise generated in a FMF by both intra- and inter-mode four wave mixing (FWM), experimentally verify the functional form of our closed form expression and use it to directly relate the potential throughput of a wavelength division multiplexed few-mode fiber transmission system to the physical fiber parameters for a system with negligible mode dependent loss. The proposed model combines the analytical integration of four wave mixing processes [19] with the velocity matched interaction between different modes [20]. We verify our hypothesis by direct measurement of four wave mixing products in a 12 mode (4 LP modes) fiber, confirming both the logarithmic dependence of FWM in a FMF and the onset of inter-mode FWM for sufficiently high WDM signal bandwidths [27]. In particular we directly observe, for the FMF used in this study, a 3 dB increase in nonlinear noise due to the onset inter-mode FWM. Finally, we interpret the implications for the design of FMFs, concluding that the optimum fiber design is likely to be independent of the majority of system and link design parameters other than the fiber itself, with the exception of the WDM signal bandwidth.

2. Analysis

Whereas recent demonstrations of FMF transmission have been over modest distances or with a low channel count [5, 28–31], for commercial use long haul systems utilizing the entire bandwidth in the wavelength domain will be required. This will significantly increase the number of velocity-matched interactions between modes [26], especially in low differential mode delay fibers [31, 32], which are envisaged to bring reduction in the digital signal

#193496 - $15.00 USD Received 8 Jul 2013; revised 15 Sep 2013; accepted 16 Sep 2013; published 20 Sep 2013

processing complexity. Velocity matching by balancing two different dispersive processes is common in nonlinear optics to maximize the efficiency of a given nonlinear process, and in this case the balance occurs between differential mode delay (DMD) and group velocity dispersion (GVD). This velocity matching process is schematically illustrated in Fig. 1 showing the calculated group delay as a function of wavelength for a four mode fiber. In a single mode fiber, it is well known that nonlinear processes such as FWM are strongly velocity matched when interacting signals are closely spaced (as will be the case within a given mode for a few mode fiber), as highlighted by the brown box in the figure. For a few-mode fiber velocity matching will also occur when chromatic and modal dispersions approximately cancel, see chain of green boxes, indicating the range of wavelengths over which a particular FWM interaction would be velocity matched. More specifically the efficiency of nonlinear interaction may be calculated for any combination of signals in any combination of modes as a function of the spacing between signals [33]. We now extend the work of [33] and [19] to derive a closed form expression for the nonlinear noise power spectral density which would be generated in a few-mode fiber.

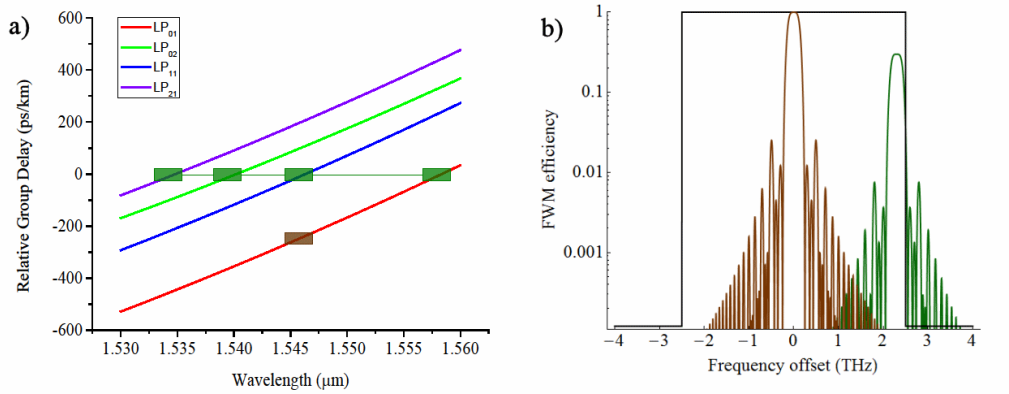

Fig. 1. (a) Calculated group delay versus wavelength for a four mode fiber showing (shaded boxes) example regions of velocity matching for intra mode (brown) and inter-mode (green) interactions. (b) Black line, a typical optical super channel spectrum; brown line FWM efficiency curves for intra-mode FWM; green line typical FWM efficiency curve for inter-mode FWM Curves are plotted from Eq. (6)for a 4 amplifier system, with an inter-mode velocity matching offset of 2.3 GHz and an exaggerated velocity-matching bandwidth of 200 GHz (for clarity).

For a periodically amplified *single-mode* transmission system with N_s identical spans and no dispersion compensation, it has been shown that in the limit of weak nonlinearity the generated nonlinear signal field E_n at frequency ω_0 in mode n is given by [34, 35];

$$E_n = \frac{\omega_0 n_2}{cA_{ijkn}} E_i E_j E_k^* \frac{1-e^{-\alpha L}e^{-j\Delta\beta_{ijkn}L}}{j\Delta\beta_{ijkn}+\alpha} \frac{\sin\left(N_S\Delta\beta_{ijkn}L/2\right)}{\sin\left(\Delta\beta_{ijkn}L/2\right)} \qquad (1)$$

where n_2 is the nonlinear refractive index, c the speed of light A_{ijkn} the effective area for the interaction between fields at frequencies $f_{i,p}$,$f_{j,q}$, $f_{k,r}$, and $f_{n,s}$ where the first subscript denotes the mode, and the second the frequency within that mode.,α represents the loss coefficient, L the span length and $\Delta\beta_{ijkn,pqrs}$ the group velocity mismatch appropriate to the interaction. Generalizing the nonlinear interaction to a multi-mode fiber is straightforward [33] and simply requires identification of the modes and frequencies associated with each of the four interacting waves denoted *i,j,k* and *n* and noting that the effective area and group velocity mismatches are given by;

#193496 - $15.00 USD Received 8 Jul 2013; revised 15 Sep 2013; accepted 16 Sep 2013; published 20 Sep 2013

$$\frac{1}{A_{ijkn}} = \frac{\iint E_i(r,\theta)E_j(r,\theta)E_k(r,\theta)E_n(r,\theta)drd\theta}{\sqrt{\iint E_i(r,\theta)drd\theta.\iint E_j(r,\theta)drd\theta.\iint E_k(r,\theta)drd\theta.\iint E_n(r,\theta)drd\theta}} \quad (2)$$

$$\Delta\beta_{ijkn} = \beta'_n + \beta'_k - \beta'_i - \beta'_j \quad (3)$$

Where r and θ are coordinates specifying the position across the transverse field $E_x(r,\theta)$ and β'_x the group delay of the x^{th} mode (were x is replaced by i,j,k or n) . For the purposes of this paper we assume that all modes have identical chromatic dispersion β'' and wavelength independent propagation constants$\tilde{\beta}_i$ such that the group velocity mismatch is given by;

$$\Delta\beta_{ijkn,pqrs} = \tilde{\beta}_n + \tilde{\beta}_k - \tilde{\beta}_i - \tilde{\beta}_j - 4\pi^2\beta''\left(f_{i,s} - f_{k,r}\right)\left(f_{j,q} - f_{k,r}\right) \quad (4)$$

where β" is the group velocity dispersion parameter, p, q, r, and s denote the frequency of the components in the i^{th}, j^{th}, k^{th} and n^{th} mode respectively. The FWM efficiency over a multi-span system as a function of the spacing between three channels in the same mode is shown by the brown curve in Fig. 1(b). This efficiency curve shows a strongly velocity matched peak for low frequency spacing and rapidly decaying weakly velocity matched peaks comprising both Maker fringes [36] and quasi velocity matching peaks [35] for wider frequency spacing. For inter-mode interactions additional walk-off due to the differential mode delay is present, significantly reducing velocity-matching and hence FWM efficiency at low frequency spacing. However, by balancing the walk-off from these two effects, efficient velocity-matching may be restored. FWM efficiency is maximized at a velocity-matched frequency offset (VMO) where the CD and DMD cancel exactly. The frequency offset (see Fig. 1) may be readily calculated from Eq. (4) to be [26]

$$\Delta f_{ijkn} = \frac{\tilde{\beta}_n + \tilde{\beta}_k - \tilde{\beta}_i - \tilde{\beta}_j}{2\pi\beta''} \quad (5)$$

For an optical super-channel with a total bandwidth B the total nonlinear noise generated by FWM between a given combination of modes may be calculated by integrating the product of curves such as those shown in Fig. 1 (Eq. (1)) with the signal power spectral density (PSD) in each mode. A closed form solution for this integral was obtained in the case of single mode fiber (corresponding to the case here where $\tilde{\beta}_n + \tilde{\beta}_k - \tilde{\beta}_i + \tilde{\beta}_j = 0$) for an OFDM superchannel with a rectangular spectrum (shown by the black curve in Fig. 1(a)) [19]. To account for all terms the integral was performed from $-B/2$ to $B/2$ where B represents the bandwidth of the WDM signal. For a few-mode fiber, in order to obtain a closed form expression, the same integral must be performed, but taking into account the VMO (Eq. (5)), and implicitly adopting the same reasonable assumptions as [19]. Simple arithmetic shows that the impact of the VMO corresponds exactly to shifting the bounds of the integral performed in [19] to $-B/2-\Delta f_{ijkn}$to $B/2-\Delta f_{ijkn}$. On one side of the velocity matching peak the integral is truncated, whilst on the other side it is extended, as is apparent by inspection of Fig. 1(b).

As the VMO increases from zero (brown curve, Fig. 1(b)), the efficiency curve shifts to one side, and as the overlap between regions of highest FWM efficiency on one side of the central velocity matching peak and the signal bandwidth decreases, so the total impact of FWM is reduced slightly, since new contributions on the opposite side are of reduced amplitude. When the frequency shift approaches half of the total occupied spectrum (green curve), contributions from the strongly velocity matched central peak are also reduced, inducing a rapid decrease in the total FWM. For even larger modal dispersions, only the tail of one set of Maker fringes contributes to the impact of the nonlinear interaction giving interaction strengths of less than 1% of that for strongly velocity matched channel combinations. In addition to the impact of the VMO, the amplitude of the generated FWM

#193496 - $15.00 USD Received 8 Jul 2013; revised 15 Sep 2013; accepted 16 Sep 2013; published 20 Sep 2013

products will also be affected by the inter-mode effective area (Eq. (2)). For a signal with a rectangular spectrum (OFDM or Nyquist WDM super channel) in each interacting mode the integral of Eq. (1) (which may be calculated by following the method of [19]) thus gives an overall efficiency parameter η_{ijkn} of:

$$\eta_{ijkn} = \frac{\xi_{ijkn}}{A_{ijkn}^2}\frac{\omega_0^2 n_2^2 N_S}{c^2 \pi \alpha |\beta''|}\left\{\ln\left(\frac{B^2+2B\Delta f_{ijkn}}{2.f_w^2}\right)+s.\ln\left(s\frac{B^2-2B\Delta f_{ijkn}}{2.f_w^2}\right)\right\} \qquad (6)$$

$$s = Sign\left(B-2\Delta f\right) \quad f_w = \sqrt{\alpha/4\pi^2\beta''}$$

where Δf_{ijkn} represents the VMO, A_{ijkn} the effective area of the interaction and ξ_{ijkn}<1 the impact of mode averaging (weakly coupling regime) [14]. For the purposes of this paper, we assume that ξ_{ijkn} = *2/3* for degenerate modes. This closed form analytical expression allows the FWM power generated in mode *i* originating from signals propagating in modes *j,k* and *l* to be calculated by taking the product of this nonlinear efficiency η_{ijkn} and the signal power spectral density, of each mode. Direct comparison of Eq. (6) with [19] will reveal that the parameter h_e from Eq. (6) has been dropped since its value is approximately unity for all practical few-mode fibers. To simplify analysis in the following sections, we define a summed nonlinear efficiency for the n^{th} mode, a_n given by:

$$a_n = \sum_{i,j,k}\eta_{ijkn} \qquad (7)$$

such that the total nonlinear power generated in the n^{th} mode is given by $a_n P_i P_j P_k$ where $P_{i,j,k}$ is the signal power spectral density in the appropriate mode.

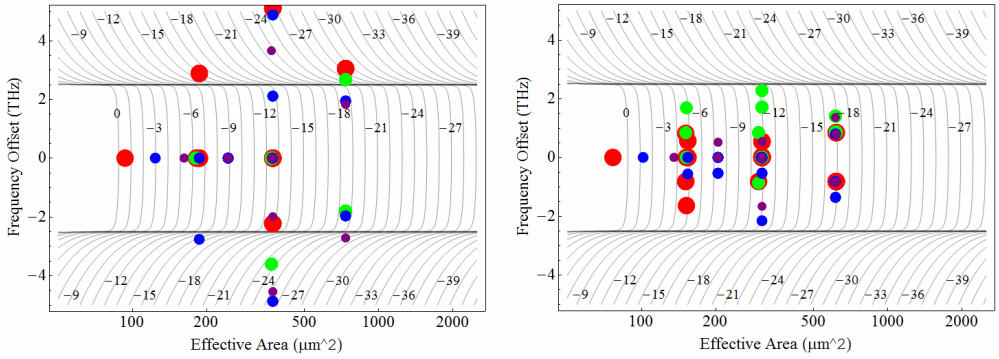

Fig. 2. Relative nonlinear noise power coefficient (in dB relative to SMF) for a step index 12-mode fiber (four LP modes) with a maximum differential mode delay of 880ps/km, 0.2 dB/km loss and assumed chromatic dispersion of 20 ps^2/km (left) and with a maximum DMD of 110ps/km (right). Contours show $10log_{10}(\eta_{ijkn})$as a function of effective area and VMO for a WDM bandwidth of 5THz. Colored dots represent the calculated values of these parameters for nonlinear noise generated in the LP_{01}(red), LP_{02}(green), LP_{11}(blue) and LP_{21} (purple) modes for different inter-mode interactions. Fiber parameters calculated using a commercial mode solver.

The implications of Eq. (6) are illustrated in Fig. 2 for two different FMF with high (left) and low (right) DMDs. Contours in Fig. 2 represent potential values of η_{ijkn} as a function the effective area and VMO. The contour plots show several important features, including (along the x-axis) the expected gradual decay in efficiency as the effective area is increased and the impact of velocity matching. As the VMO increases gradually from zero the nonlinear efficiency decays slightly as Maker fringes fall outside the WDM signal bandwidth. Eventually, when the VMO approaches half the WDM signal bandwidth, the main lobe (see Fig. 1(b)) falls outside the WDM signal bandwidth, inducing a rapid drop in η_{ijkn}. In the

#193496 - $15.00 USD Received 8 Jul 2013; revised 15 Sep 2013; accepted 16 Sep 2013; published 20 Sep 2013

example shown this results in a sharp discontinuity at a VMO of ± 2.5 THz (signified by the closely spaced contour lines). The frequency offset at which this rapid decay occurs is determined primarily by the signal bandwidth (5 THz in this case), the reminder of the shape is determined by the phase matching parameter f_w and the signal bandwidth. Scaling (normalized in the figure) depends on a number of other fiber parameters, as detailed in Eq. (6). Of course, for any given fiber, only certain combinations of VMO and effective area are possible. The dots in Fig. 2 represent values of η_{ijkn} for different interactions (combinations of modes i,j,k, n) for two specific fibers The dots are color coded according to the mode degraded by the interaction in question (n), the size of the dots are varied simply to enhance visibility of overlapping, or nearly overlapping, points. For each fiber, there are a number of interactions (each with its own effective area and VMO and illustrated by one of the dots) which fall within the high efficiency region (between ± 2.5 THz), including intra-modal effects and partially degenerate inter-mode effects. A number of other FWM interactions clearly exist which are also strongly velocity matched. Comparing the two fibers in Fig. 2, it is apparent that reducing the differential mode delay increases the number of these additional velocity matched interactions. For the higher DMD fiber there are a number of weakly velocity matched interactions (outside the VMO region bounded at ± 2.5 THz), which will be of increased importance if the signal bandwidth B is extended allowing strong velocity matching at greater VMO (resulting in a movement of the discontinuity in Fig. 2).

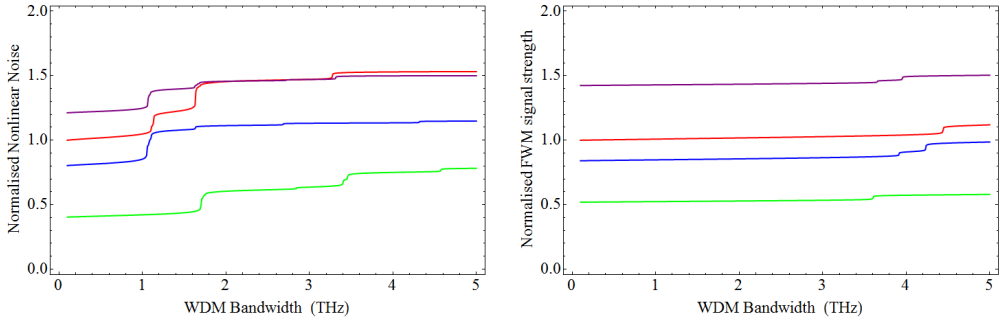

Fig. 3. Nonlinear noise power normalized to LP_{01} mode at 100GHz bandwidth as a function of WDM signal bandwidth for the high (left) and low (right) DMD fibers of Fig. 2. LP_{01} (red), LP_{02} (green), LP_{11} (blue) and LP_{21} (purple).

To calculate the total nonlinear noise influencing a given mode, all of the interactions influencing that mode must be summed (Eq. (7)). This corresponds to summing the contributions from each of the colored points associated with that mode in Fig. 2 (or the equivalent figure for fiber in question). This is illustrated in Fig. 3 which shows the nonlinear noise power generated at the center of the WDM versus the WDM bandwidth for these two four LP mode fibers. A number of discontinuities are apparent, in addition to the logarithmically increasing background expected for a SMF [37], with larger number of discontinuities observed for the fiber with the lowest DMD giving a significant increase in the overall nonlinear power spectral density. These discontinuities correspond to the signal bandwidth becoming sufficiently large to result in an additional strongly velocity matched contribution to the total nonlinear noise (see the green curve in Fig. 1(b), showing a WDM bandwidth just beyond such a discontinuity). In terms of Fig. 2, as the WDM bandwidth is increased, the discontinuity (at ± B/2) moves to higher VMO, allowing strong contributions from different points.

3. Experimental verification

We confirmed the predictions of Eq. (6) using the following simple measurement (Fig. 4(top) with a 30km low DMD FMF similar to the fiber used in [31]. A gain-flattened erbium doped

#193496 - $15.00 USD Received 8 Jul 2013; revised 15 Sep 2013; accepted 16 Sep 2013; published 20 Sep 2013

fiber amplifier (GFA) was used as a source of amplified spontaneous emission (ASE), which was shaped into a rectangular spectral blocks, representing highly dispersed WDM signals, using a wavelength selective switch (WSS). These blocks were amplified by a 38dBm GFA and the WSS was re-adjusted to ensure a uniform power spectral density. The central 50GHz section of the ASE spectrum was attenuated using the WSS in order to allow monitoring of the FWM signal. The FMF launch was adjusted by offsetting the position of the single mode fiber to maximize nonlinear mixing between the LP_{01} and LP_{11} modes, (giving a total excess coupling loss of 1.5dB). The output comprised coupling lenses, collimator and a phase plate, had an excess loss of ~5dB. The LP_{01} and LP_{11}fiber modes were selected using the appropriate phase plate (only one orientation used for LP_{01}) and the output spectrum recorded using an optical spectrum analyzer connected via a single mode fiber patch cord. The spectrum was used to determine the output power spectral density (and by implication the relative input power spectral density) and the FWM power generated in the central notch. To cover the full measurement the pump power of the second GFA was reduced to achieve a constant power spectral density. Three overlapping sets of data were obtained at different target power spectral densities.

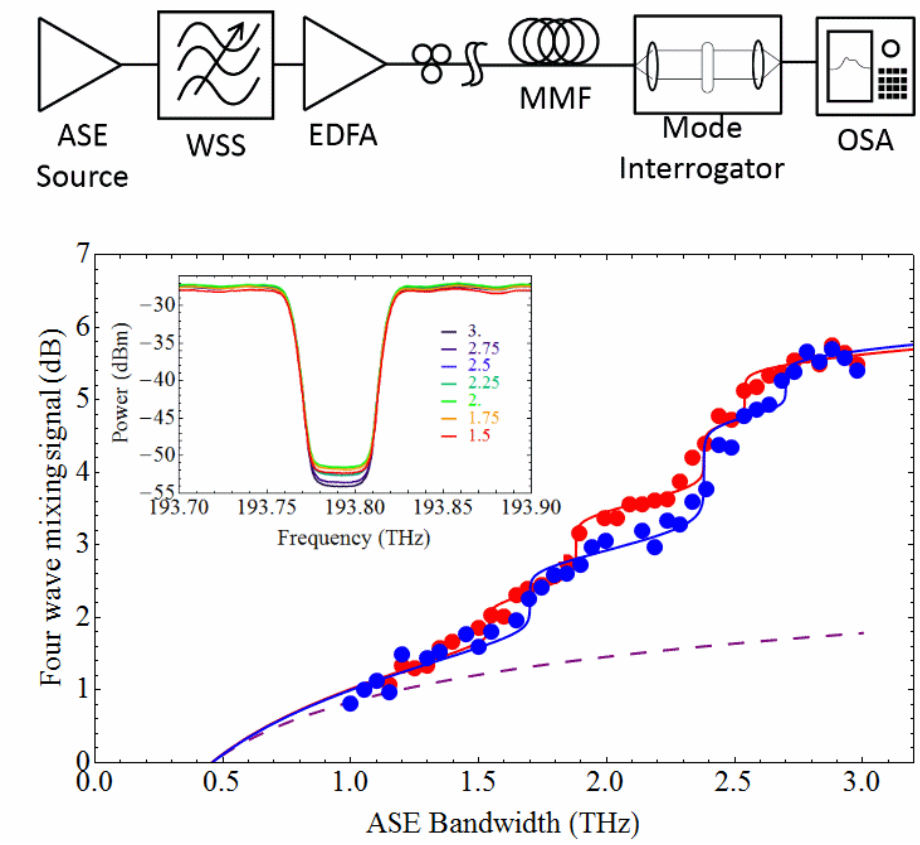

Fig. 4. *(top)* Experimental configuration used to measure few mode fibers (lenses and positioning stages at the ends of the few mode fiber are omitted for clarity). (*bottom*) Comparison of theoretical (solid lines) and experimental (dots) results for the LP_{01}(red) and LP_{11} (blue) mode showing the normalized nonlinear power spectral density at the center of the band as a function of the bandwidth of an amplified spontaneous emission source with a 50GHz frequency notch at the center. Theoretical predictions are based on typical measured DMD from the same fiber draw as the fiber used in this experiment [17], also shows theoretical prediction neglecting the inter mode nonlinearity (dotted lines)and typical output spectra (inset for signal widths between 1.5 (red) and 3 (dark blue) THz).

#193496 - $15.00 USD Received 8 Jul 2013; revised 15 Sep 2013; accepted 16 Sep 2013; published 20 Sep 2013

Figure 4(bottom) shows the measured FWM efficiency, calculated by dividing the output PSD measured in the central 50 GHz gap using an optical spectrum analyzer (and induced by FWM) by the cube of the input PSD calculated from the output PSD measured in the 200 GHz regions either side of the central 50 GHz gap and corrected for the fiber loss. The measurement was performed for both the LP_{01} and LP_{11}modes, with the inset to Fig. 4(bottom) showing typical recorded output spectra (zoomed in around the central notch) for a range of ASE widths. The inset shows the FWM signal in the gap around 193.79 THz growing as a function of the overall spectral width of the ASE, whilst the input signal amplitude remains approximately constant (see spectral regions between 193.7 and 193.75THz and between 193.83 and 193.9 THz). The resultant data was normalized (arbitrarily) to the efficiency obtained for a 1GHz ASE bandwidth. The results show the expected logarithmic growth trend, punctuated by discrete steps corresponding to the onset of individual inter mode interactions in excellent agreement with theoretical predictions based on summing Eq. (6) over all mode combinations. The fit shown was achieved for VMOs of 0.8, 0.9 and 1.2 ± 0.1 THz (LP_{01}) and 0.85, 1.2 and 1.35 ± 0.1 THz (LP_{11}). The fitting parameters suggest inter-mode interaction strengths of around 15% of the intra-mode strength, representing effective areas around 2.5 times greater than the LP_{01} intra-mode effective area, which is consistent with the overlap integrals for a typical four mode fiber. Of particular significance to the analysis of communication systems, we observe that for signal bandwidth beyond 2.5 THz, the total FWM signal more than 3dB greater than expected from intra-mode nonlinearity alone (purple dotted line). This would be expected to reduce the total information spectral density of a fiber link by approximately 2b/s/Hz in the limit of a high signal to noise ratio (SNR) [3].

4. Capacity limits of few mode fiber systems

Having experimentally verified a method to accurately predict the nonlinear noise power generation, the capacity limits may be estimated. For SMF, calculation of the equivalent nonlinear efficiency parameter η_{iiii} [19] provides accurate performance estimations [38] of the so called "nonlinear Shannon limit". Channel capacity calculations used to derive the conventional "Shannon limit" require rigorous calculations of the mutual information between transmitter and receiver. To avoid confusion with such calculations, whilst allowing comparison with other works on "nonlinear Shannon limits" based on the calculation of noise fields, we introduce the phrase nonlinear information spectral density (ISD_{NL}). In addition to the assumptions of [19] we make the following assumptions; (1) that sufficient CD and DMD to randomize span-to-span nonlinear interactions, and that random mode coupling equalizes launch powers and randomizes contributions from each mode [14], that is, whilst the mode coupling is in the weakly-coupled regime, it is sufficiently strong to scramble the modes at the output of a fiber span, (2) there is *no* compensation of nonlinearity (inter or intra channel), (3) as a consequence of (2) contributions to the nonlinear noise from interactions between signal and noise may be neglected, (4) that mode coupling equalizes the launch power for each mode and (5) that mode dependent loss is negligible. Considering these assumptions the achievable ISD_{NL} can be recalculated for a FMF by considering the various interactions which may be velocity-matched within the signal bandwidth and summing over all modes. However, unlike single mode fiber [23], practical nonlinearity compensation has yet to be proposed for few mode fibers, and so we calculate ISD_{NL} omitting the correction term which accounts for nonlinearity compensation [25].

$$ISD_{NL} = \sum_{n=1}^{M} \log_2 \left(1 + \frac{P_s}{P_N + \sum_{i,j,k} \eta_{ijkn} P_s^3} \right) \tag{8}$$

#193496 - $15.00 USD Received 8 Jul 2013; revised 15 Sep 2013; accepted 16 Sep 2013; published 20 Sep 2013

where P_s and P_N are the signal and accumulated noise power spectral densities per mode respectively. Equation (6) and Eq. (8) may then be used to calculate the nonlinear information spectral density of a given multi-mode fiber, where P_N is the amplified spontaneous emission power spectral density at the end of the link (including a final amplification stage) and P_S the signal power spectral density per mode at the output of each amplifier. For large signal to noise ratios, algebraic manipulation of Eq. (8), using the simplification of Eq. (7) enables the relative ISD_{NL} of MxM MIMO operation of a multimode fiber to be expressed as:

$$ISD_{NL}\Big|_M = M\left(\frac{C}{B}\Big|_1\right) - \log_2\left[\prod_{n=1}^{M}\left(\frac{2}{3}\frac{P_1}{P_M} + \frac{1}{3}\frac{a_n P_M^2}{a_1 P_1^2}\right)\right] \tag{9}$$

where P_1 is the optimum power spectral density when the fiber is operated in a single LP mode (assuming zero mode coupling), P_M the optimum power spectral density when all M modes are utilized and a_1 and a_M the equivalent total nonlinear efficiencies respectively (calculated using Eq. (7)) The optimum power spectral density may be calculated from the analytical solution to

$$M = \sum_{i=1}^{M}\frac{3a_i P_M^3}{\left(P_N + a_i P_M^3\right)} \tag{10}$$

recalling that P_N represents the accumulated ASE power spectral density. Equation (9) reveals the expected M-fold increase in capacity but with a small reduction from the re-optimization of the optimum signal power spectral density, reduced slightly by the additional nonlinear terms, readily calculated from Eq. (10), and the relative FWM strength a_1. The capacity is also directly influenced by the effective area of the fundamental mode through the first term in Eq. (6). Figure 5(a) shows the familiar non-linear information spectral density curve for different four mode fiber designs. For any given fiber, the difference in performance for each mode is small. The fibers represent examples of high and low DMD FMFs with modest fundamental mode effective areas, and a low DMD fiber with a low fundamental mode effective area. Clearly both the overall effective area and the DMD have a direct influence on the maximum capacity of the system. Each mode exhibits a slightly different nonlinear threshold (Eq. (10) calculates the overall optimum launch condition), suggesting that some advantage may be obtained from individually optimizing the relative launch power for each mode [39], either at the transmitter for sufficiently weakly coupled fibers or after amplification, provided the benefit outweighed the increase in outage probability [7]. Note that the reference of fundamental mode propagation used here may be replaced by a conventional single mode fiber by replacing P_1 and a_1 with the appropriate values for the reference fiber, for example P_{SMF} and a_{SMF}.

#193496 - $15.00 USD Received 8 Jul 2013; revised 15 Sep 2013; accepted 16 Sep 2013; published 20 Sep 2013

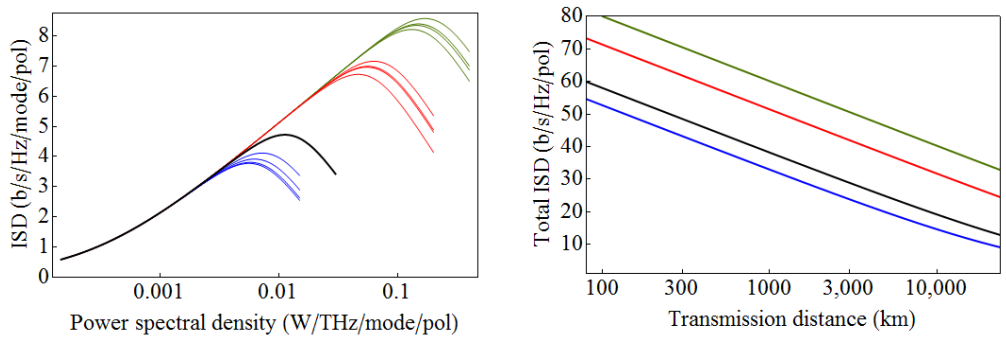

Fig. 5. (left) ISD versus signal power spectral density for different four-mode fibers (separate line for each mode) calculated according to Eq. (9) and (right) total capacity for the four FMF systems obtained by summing the ISDs of all modes at the optimum PSD. Both figures show ISD for SMF (black),high effective area step index FMF (green), high effective area graded index FMF (red), small effective area graded index FMF) (blue) (DMDs shown in Table 1). Left figure shows ISD per mode, right figure shows total ISD (of six fibers for SMF). Systems have 80km amplifier spacing (4.8dB noise figure), 100 channels (50GHz spacing, assuming OFDM or Nyquist signaling), 0.2dB loss and dispersion (β'') of 20ps^2/km.

Table 1. Effective areas and differential mode delays of fibers used to calculate ISD variations of Fig. 5

Fiber Designation	Effective Area of LP_{01} (μm^2)	Index Profile	Differential Mode Delay		
			DMD LP_{02}-LP_{01} (ps/km)	DMD LP_{11}-LP_{01} (ps/km)	DMD LP_{21}-LP_{01} (ps/km)
Green*	11,000	Step	74	46	89
Red	2,000	Graded	346	237	444
Blue	63	Graded	–92	37	10
Black	88	Step	N/A	N/A	N/A

*Fiber not feasible due to high bending losses.

Figure 5 (right) illustrates the performance of each fiber type as a function of system length, plotting the total capacity instead of the information spectral density per mode using Eqs. (6) and (8). Whereas the actual performance is dependent on the optical SNR, the difference in ISD between fiber types appears to be largely independent of the system length for all practical scenarios, only noticeably varying for transmission distances around 20,000km in this example. This may be understood by inspecting Eq. (9), where we may observe that the penalty arising from inter-mode nonlinear effects contains no length dependence (all length dependent terms such as a_M appear as ratios). Of course, the high signal to noise ratio approximation breaks down for the longest transmission distances, as illustrated by the slight convergence of the curves in Fig. 5 (right) beyond 10,000km. We may thus conclude that in the limit of a typical optical signal to noise ratio, the relative performance of different fiber designs depends only on the fiber design itself and on the WDM bandwidth. We may thus optimize a fiber design using the analytical method described here considering only a typical transmission system. A typical design choice is considered in Fig. 6, where we plot the total ISD, at the optimum power spectral density, for a system using a trench assisted graded index FMF of constant core diameter. To obtain the plot, the refractive index curvature and magnitude were varied and we plot the results for values which realized four mode fibers as a function of their maximum DGD (difference between fastest and slowest modes).The capacity clearly reduces monotonically with decreasing DMD favoring large DMD values for optimum nonlinear performance. Since small DMDs are preferred to minimize digital signal processing overheads, the ability to calculate the capacity and optimize the compromise is paramount.

#193496 - $15.00 USD Received 8 Jul 2013; revised 15 Sep 2013; accepted 16 Sep 2013; published 20 Sep 2013

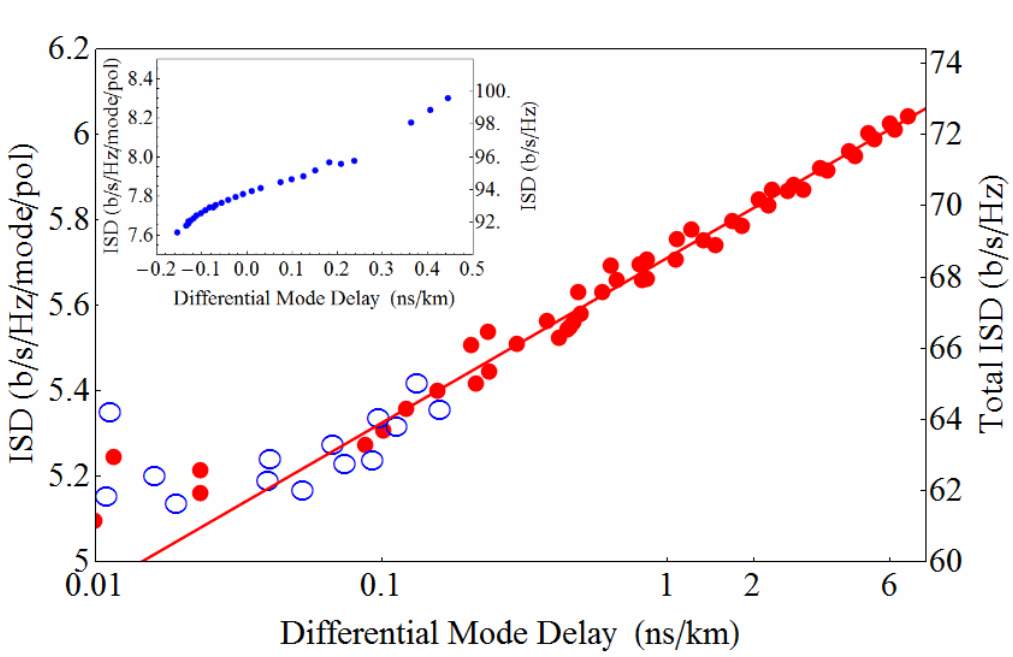

Fig. 6. Predicted maximum total information spectral density (right axis) and information spectral density per mode (left axis) for trench assisted fiber designs with a core radius of 10.4 μm as index curvature is varied resulting in differences in DMD, plotted as a function of resultant DMD between LP01 and LP21 for positive (red filled circles) and negative values (**blue open circles**). Inset shows a similar fiber with a core radius of 30 μm (filled blue circles). Solid red line shows a logarithmic fit over points falling within 0.1 and 8 ns/km DMD as a guide to the eye. Both plots are for a 3,200km system with 80km amplifier spacing (4.8dB noise figure), 100 channels (50GHz spacing), 0.2dB loss and dispersion (β'') of 20ps^2/km.

The inset to Fig. 6 shows a different fiber design, with an increased core diameter, again with the refractive index curvature varied. As expected the overall ISD scales with the increased core area. Our results suggest that effective area dominates over the effect of reduced differential mode delay, although effects such as bend loss and mode dependent loss have been neglected in this preliminary study. This direct dependence of effective area is illustrated in Fig. 7, which shows the variation in predicted ISD for various step-index fibers as the core radius and refractive index are simultaneously varied such that four LP modes are supported for each fiber.

Combining analytical result of the potential ISD predicted by the approach of this paper with calculations of digital signal processing complexity [40] should enable fibers to be designed to which optimize the tradeoff between signal processing complexity (proportional to DGD) and nonlinearity without the need for extensive numerical simulations. Since our preliminary results suggest that the system reach, amplifier noise figure etc. do not influence the relative performance of different fiber designs, such an optimization should be possible without detailed knowledge of the precise system configuration.

#193496 - $15.00 USD Received 8 Jul 2013; revised 15 Sep 2013; accepted 16 Sep 2013; published 20 Sep 2013

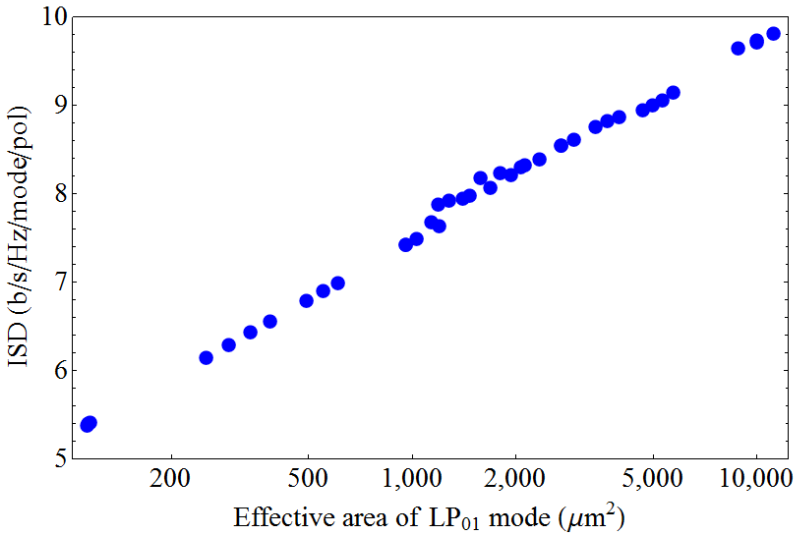

Fig. 7. Predicted information spectral density per mode for step index fiber designs supporting four LP modes, plotted as a function of resultant LP_{01} effective area. System parameters correspond to a 3,200km system with 80km amplifier spacing (4.8dB noise figure), 100 channels (50GHz spacing), 0.2dB loss and dispersion (β") of 20ps^2/km.

5. Conclusions

In this paper we have proposed closed form expressions to calculate the nonlinear information spectral density of a multi-mode fiber system. We have shown that the approach accurately predicts experimental measurements. These experimental results suggest that for signal bandwidths above 2.5 THz inter-mode FWM is likely to induce an increase in nonlinear noise of around 3dB and a corresponding reduction in overall fiber information spectral density of a few b/s/Hz (around 10%). We have presented a selection of results which show that the maximum potential ISD decreases with decreasing DMD and that for practical cases the decrease in ISD does not depend on the system design.

Acknowledgments

This work was partly funded by the European Communities 7th Framework Programme FP/2007-2013 (Grant 258033-MODE-GAP), EPSRC (Grant EP/J017582/1-UNLOC), Science Foundation Ireland (Grants 06/IN/I969 and 10/CE/I1853) and The Royal Society (Grant WM120035-TEST).

#193496 - $15.00 USD Received 8 Jul 2013; revised 15 Sep 2013; accepted 16 Sep 2013; published 20 Sep 2013